in vivo *37*: 2498-2509 (2023)
doi:10.21873/invivo.13357

Effects of Comano Spring Water-derived Bacterial Lysates on Skin Regeneration: An *Ex-vivo* Study

GIOVANNI NICOLETTI[1,2,3], MARCO SALER[1,2], MARCO MARIO TRESOLDI[1,2], LAURA VILLANI[4], ERIKA MARIA TOTTOLI[5], OLIVIER JOUSSON[6,7] and ANGELA FAGA[2]

[1]*Plastic and Reconstructive Surgery, Department of Clinical Surgical, Diagnostic and Pediatric Sciences, University of Pavia, Pavia, Italy;*
[2]*Advanced Technologies for Regenerative Medicine and Inductive Surgery Research Center, University of Pavia, Pavia, Italy;*
[3]*Surgery Unit, Azienda Socio-Sanitaria Territoriale di Pavia, Pavia, Italy;*
[4]*Pathological Anatomy and Histology Unit, Istituti Clinici Scientifici Maugeri SB SpA IRCCS, Pavia, Italy;*
[5]*Laboratory of Pharmaceutical Technology and Law, Department of Drugs Science, University of Pavia, Pavia, Italy;*
[6]*Interdepartmental Center of Medical Sciences (CISMED), University of Trento, Trento, Italy;*
[7]*Department of Cellular, Computational and Integrative Biology (CIBIO), University of Trento, Trento, Italy*

Abstract. *Background/Aim: A native non-pathogenic bacterial microflora was identified in Comano (TN, Italy) spring water. The aim of this study was to investigate the regenerative effects of some of the bacterial lysates extracted from this water in a human ex-vivo skin experimental wound model. Materials and Methods: Bacterial lysates were extracted from four new isolates: lysate 1 (L1) - closest relative Rudaea cellulosilytica, phylum Proteobacteria; lysate 2 (L2) - closest relative Mesorhizobium erdmanii, phylum Proteobacteria; lysate 3 (L3) - closest relative Herbiconiux ginseng, phylum Actinobacteria; lysate 4 (L4) - closest relative Fictibacillus phosphorivorans, phylum Firmicutes. Their regenerative effects were investigated in a human ex-vivo skin experimental wound healing model at 3 (T1), 5 (T2), and 10 days (T3). Results: The samples cultured with the L2 lysate displayed both an earlier and complete restoration of all the skin layers and their features were the closest to the normal skin. The regenerated epidermis demonstrated a complete maturation as the normal epidermis. The papillary dermis appeared mature, and the reticular dermis displayed both collagen and elastic fibres regularly parallel to the skin surface. An anti-inflammatory effect was displayed by the L1 lysate, but this action did not constitute a regenerative effect, suggesting that pathways for inflammation and regeneration might be different. Conclusion: The therapeutic power of spring waters is not exclusively related to their mineral composition, but it may also be attributable to their native non-pathogenic bacterial microflora.*

Correspondence to: Giovanni Nicoletti, MD, FEBoPRAS, Plastic and Reconstructive Surgery, Department of Clinical Surgical Diagnostic and Pediatric Sciences, University of Pavia, Viale Brambilla, 74, 27100 Pavia, Italy. Tel: +39 0382984184, Fax: +39 0382984055, e-mail: giovanni.nicoletti@unipv.it

Key Words: Regeneration, microbiota, spring water, *ex-vivo*, skin culture, skin models.

The favourable regenerative effects of some spring waters on wound healing have long been empirically demonstrated (1-5). Over the last decade, our research group investigated Comano (TN, Italy) spring water and demonstrated its skin regenerative properties both in *in-vitro* human fibroblast cultures and in an *ex-vivo* human experimental skin wound model (6, 7). A rich, native, non-pathogenic bacterial microflora was demonstrated in this spring water (8). Further genetic investigations and classification of the latter microbial flora was carried out by Pedron *et al.* (9). It demonstrated an anti-inflammatory effect of some native bacterial strains in this water and extracted their metabolic products as bacterial lysates. We investigated four of these bacterial lysates on human fibroblast *in-vitro* cultures and demonstrated strain-specific regenerative properties (10). The aim of this study was to investigate the regenerative effects of the same bacterial lysates in a human *ex-vivo* skin experimental wound model.

Materials and Methods

The project was conducted in cooperation with the Plastic and Reconstructive Surgery Unit of the Department of Clinical-Surgical, Diagnostic and Pediatric Sciences, the Advanced Technologies for Regenerative Medicine and Inductive Surgery Research Center, the Immunology and General Pathology Laboratory of the Department of Molecular Medicine of the University of Pavia (Italy), the Pathological Anatomy Section Laboratory of the ICS Maugeri SB SpA IRCCS in Pavia (Italy), the Laboratory of Microbial Genomics of the Department of Cellular, Computational and Integrative Biology (CIBIO) of the University of Trento (Italy) and the G.B. Mattei Institute in Comano (TN, Italy).

The experiments were carried out between April 2018 to January 2020. The study was approved by the Ethics Committee of the ICS Maugeri SB SpA IRCCS, Pavia (Italy) (project identification code, 2064) on 26 September 2016. The study conformed to the 1975 Declaration of Helsinki and informed written and signed consent was obtained from all of the patients.

Bacterial isolation, identification, selection, and preparation of the bacterial lysates. The bacterial isolation, identification and selection and the preparation of the bacterial lysates were performed at the Laboratory of Microbial Genomics of the Department of Cellular, Computational and Integrative Biology (CIBIO) of the University of Trento (Italy) using the same methods as a previous study, which examined the effect of the same bacterial lysates on human fibroblast *in-vitro* cultures (10). The selected bacterial lysates were as follows. Lysate 1 (L1) had an isolate code of 3F27F6 and an average nucleotide identity (ANI) value of 82.6% - closest relative *Rudaea cellulosilytica* of the phylum *Proteobacteria*. Lysate 2 (L2) had an isolate code of 3P27G6 and an ANI value of 86.5% - closest relative *Mesorhizobium erdmanii* of the phylum *Proteobacteria*. Lysate 3 (L3) had an isolate code of 3FA27C10 and an ANI value of 83.1% - closest relative *Herbiconiux ginseng* of the phylum *Actinobacteria*. Lysate 4 (L4) had an isolate code of E and an ANI value of 89.8% - closest relative *Fictibacillus phosphorivorans* of the phylum *Firmicutes*.

Study design. The human specimen collection and processing, and the study design were identical to those of a previous study on filtered Comano spring water with the same human *ex-vivo* skin experimental wound model (7, 11). Human skin samples were collected in the Operating Rooms of the ICS Maugeri. The samples were obtained from anatomical specimens harvested during sessions of reduction mammoplasty or abdominoplasty, performed on 12 healthy female patients with an age range of 40-50 years.

The specimens were processed in the Immunology and General Pathology Laboratory of the Department of Molecular Medicine of the University of Pavia in a sterile environment with a second-class laminar flow hood. Each skin sample was then divided into 16 fragments measuring 1 cm in diameter. One fragment out of the 16 was sent for morphological analysis to assess the histological features of the untreated skin (US) using the staining methods described below. The remaining 15 fragments were punctured in their central portion with a sterile 3 mm circular punch to establish a skin loss in each sample as described previously (7, 11, 12). The punctured specimens were placed in Transwell inserts of 24-well, multiwell plates (membrane pore size, 0.40 μm; Constar insert, 0.33 cm^2; Corning Incorporated, Corning, NY, USA).

Table I. *Semi-quantitative analysis of the cellular features.*

		T1	T2	T3
C	Epithelial cell advancement front	+	++	++
	Multi-layered re-epithelialisation	+	++	++
	Ki-67-positive nuclei	+	+	++
	Lymph-plasma-cell infiltration	+	+	++
	Fibroblast infiltration	+	+	++
	Vascularisation	+	+	+
L1	Epithelial cell advancement front	+	++	++
	Multi-layered re-epithelialisation	+	++	++
	Ki-67-positive nuclei	++	0	+
	Lymph-plasma-cell infiltration	0	+	0
	Fibroblast infiltration	0	+	+
	Vascularisation	+	+	+
L2	Epithelial cell advancement front	++	++	+++
	Multi-layered re-epithelialisation	++	++	+++
	Ki-67-positive nuclei	++	+	+
	Lymph-plasma-cell infiltration	+	++	++
	Fibroblast infiltration	+	++	+
	Vascularisation	+	+	+
L3	Epithelial cell advancement front	+	++	+++
	Multi-layered re-epithelialisation	++	0	++
	Ki-67-positive nuclei	0	++	++
	Lymph-plasma-cell infiltration	++	+	++
	Fibroblast infiltration	+	+	+
	Vascularisation	+	+	+
L4	Epithelial cell advancement front	+	++	+++
	Multi-layered re-epithelialisation	+	+	++
	Ki-67-positive nuclei	0	+++	+++
	Lymph-plasma-cell infiltration	+	++	+
	Fibroblast infiltration	+	+	+
	Vascularisation	+	+	+

C: Control; L1: Lysate 1; L2: Lysate 2; L3: Lysate 3; L4: Lysate 4; Epithelial cell advancement front: 0: absent; +: initial; ++: advanced; + + +: complete; Multi-layered re-epithelialization: 0: absent; +: low; ++: good; + + +: mature; Ki-67-positive nuclei: 0: absent; +: present at the margins; ++: diffuse; + + +: abundant; Lymph-plasma-cell infiltration: +: minimum; ++: moderate; + + +: abundant; Fibroblast infiltration: +: minimum; ++: moderate; + + +: abundant; Vascularization: +: poor; ++: discrete; + + +: abundant.

The 15 centrally punctured skin specimens were used to harvest both paired control and experimental samples. The three control samples were cultured in DMEM (DMEM powder with 4500 mg/l glucose, 0.584 g/l L-glutamine, and 0.11 g/l sodium pyruvate) (Sigma-Aldrich, Merck KGaA, Darmstadt, Germany), which was reconstituted with distilled water (Milli-Q, Merck-Millipore, Darmstadt, Germany) and enriched with 3.7 g/l sodium bicarbonate, 10% foetal bovine serum, 1% (10,000 U/ml) penicillin, and streptomycin (10 mg/ml) (all from Sigma-Aldrich), and the central skin loss region was treated with a constant volume (20 μl) of sterile saline solution.

The 12 experimental samples followed 4 different lines. All of them were cultured in DMEM and the samples in each line had the central skin loss region treated with 0.33% suspension of each of the four bacterial lysates reconstituted with distilled water. Following treatment, both the control and the experimental samples were incubated at 37˚C (T0).

The culture medium was replaced every two days while, inside the central skin loss, the different solutions were topped daily up to the 10th day. A morphological analysis was carried out on the control samples and on the four different experimental ones at 3 (T1), 5 (T2), and 10 days (T3).

Assessment modalities. Morphological Analysis was performed at the Pathological Anatomy Section Laboratory of the ICS Maugeri using the haematoxylin and eosin, Masson's Trichrome, Weigert and Ki-67 stainings as in a previous study with the same human *ex-vivo* skin experimental wound model (11).

Results

The results are comprehensively summarised in Table I and Table II. Haematoxylin and Eosin staining is shown in Figure 1.

Control (C). Re-epithelialisation. The control samples displayed a progressive advancement and multi-layered organisation of the re-epithelialisation front at each observation time point although, at T3, the central injury failed to be fully covered by an epithelial lining and the stratum corneum was missing. The keratinocytes in the basal layer displayed a pigmentation due to intracellular melanin.

Cellular infiltration. An inflammatory cell infiltration, represented by lymphocytes and plasma cells, was minimal at T1 and T2, although at the latter time point cell infiltration was mainly observed around the blood vessels. At T3 the inflammatory cell infiltration moderately increased and displayed an even distribution.

The fibroblast infiltration increased progressively with time. Nevertheless, at T1 and T2 it was minimal, and it was mainly observed in the papillary dermis. At T3, the fibroblast infiltration increased *vs*. the previous time points and was mainly distributed in the reticular dermis.

Vascularisation. A scarce vascularisation was observed at all observation time points.

Dermal structure. From T1 to T2, the papillary dermis displayed an early and progressive development, moving from the peripheral injury margins towards the centre of the wound. At T3, a more structured papillary dermis was appreciated. The reticular dermis appeared well structured with reduced inter-fibrillary spaces at all observation time points. A blend of thin and thick collagen fibres was seen at T1 and T2. A generalised thickening of collagen fibres was seen at T3 *vs*. the previous times. The collagen fibres displayed a chaotic orientation at T1, while at T2 they displayed a somewhat perpendicular orientation to the skin surface. The latter was clearly appreciated at T3.

Table II. *Semi-quantitative analysis of the connective tissue features*.

		T1	T2	T3
C	Papillary dermis	0	+	++
	Reticular dermis	++	++	++
	Masson's trichrome blue stained collagen fibres' thickness	++	++	+++
	Reticular collagen fibres' orientation	+	++	++
	Elastic fibres' amount	+	+	+
	Elastic fibres' integrity	++	+	++
	Elastic fibres' orientation	++	++	+++
L1	Papillary dermis	0	+	+
	Reticular dermis	+	++	+
	Masson's trichrome blue stained collagen fibres' thickness	+	++	++
	Reticular collagen fibres' orientation	+	++	+++
	Elastic fibres' amount	++	+++	+++
	Elastic fibres' integrity	++	++	++
	Elastic fibres' orientation	+++	++	++
L2	Papillary dermis	+	+	+++
	Reticular dermis	+	+++	+++
	Masson's trichrome blue stained collagen fibres' thickness	++	++	++
	Reticular collagen fibres' orientation	+++	++	+++
	Elastic fibres' amount	+++	+++	+++
	Elastic fibres' integrity	++	++	++
	Elastic fibres' orientation	+	++	+++
L3	Papillary dermis	0	+	+
	Reticular dermis	+	++++	++
	Masson's trichrome blue stained collagen fibres' thickness	++	+++	++
	Reticular collagen fibres' orientation	+	++	+
	Elastic fibres' amount	+	+	+
	Elastic fibres' integrity	+++	+++	++
	Elastic fibres' orientation	++	+	+
L4	Papillary dermis	0	+	++
	Reticular dermis	+	++	+++
	Masson's trichrome blue stained collagen fibres' thickness	++	++	+++
	Reticular collagen fibres' orientation	+	+	++
	Elastic fibres' amount	+	+	++
	Elastic fibres' integrity	+	+++	+++
	Elastic fibres' orientation	+	++	+++

C: Control; L1: Lysate 1; L2: Lysate 2; L3: Lysate 3; L4: Lysate 4; Papillary dermis: 0: absent; +: initial; ++: advanced; + + +: mature; Reticular dermis: +: very loose; ++: partially loose; + + +: thick; + + ++: hypertrophic; Masson's trichrome blue collagen fibres' thickness: +: thin fibres; ++: blended thin and thick fibres; + + +: thick fibres; + + ++: very thick fibres; Reticular collagen fibres' orientation: +: chaotic; ++: perpendicular to the skin surface; + + +: parallel to the skin surface; Elastic fibres' amount: +: minimal; ++: moderate; + + +: abundant; Elastic fibres' integrity: +: fragmented fibres; ++: blended fragmented and long fibres; + + +: long fibres; Elastic fibres' orientation: +: poorly organized; ++: perpendicular to the skin surface; + + +: parallel to the skin surface.

Lysate 1. Re-epithelialisation. The epithelial front advancement and structure at all observation times was the same as the controls. Nevertheless, the basal keratinocytes did not display any melanin pigmentation.

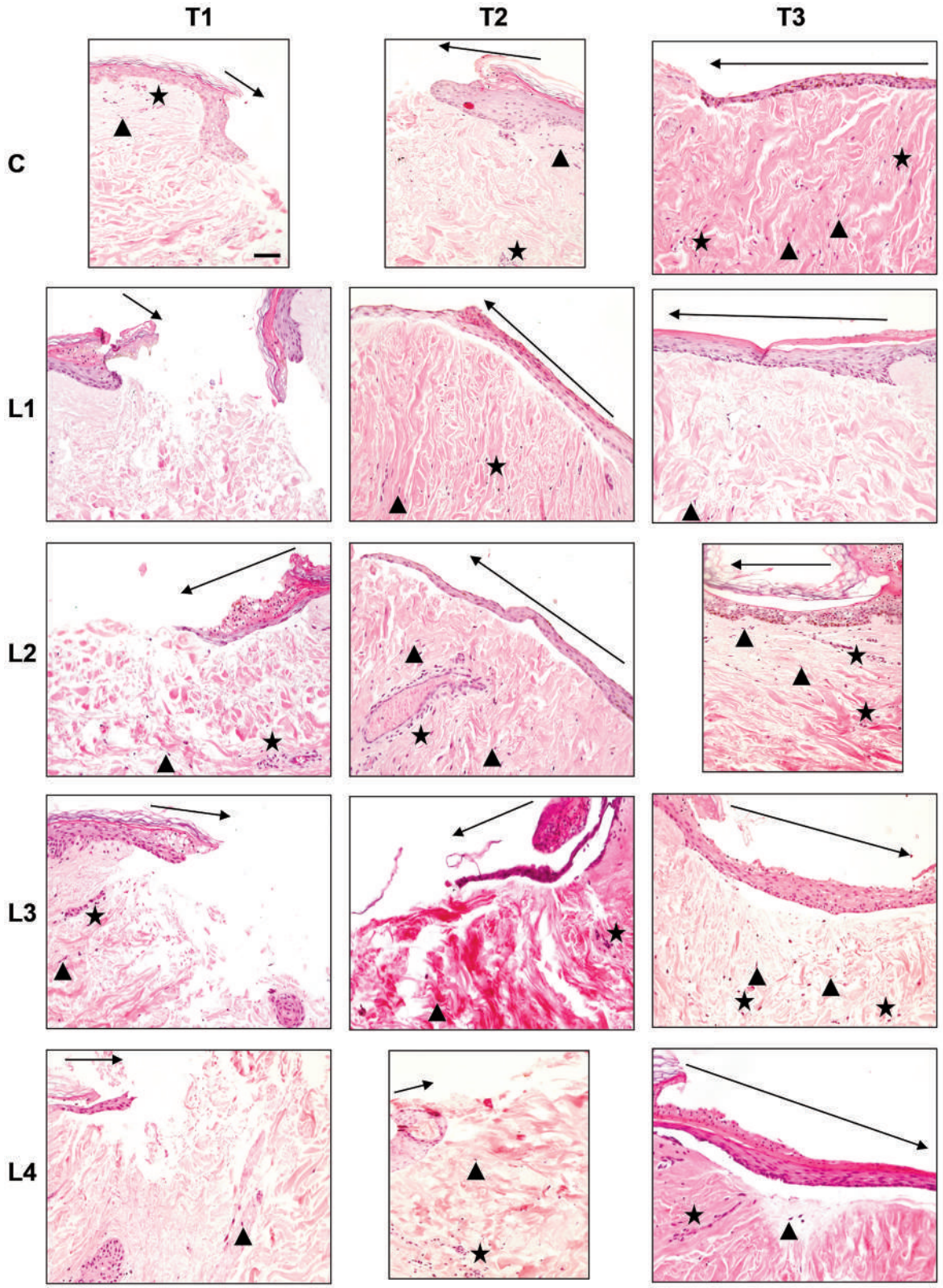

Figure 1. *Haematoxylin and eosin staining in the different culture conditions (C: Control; L1: Lysate 1; L2: Lysate 2; L3: Lysate 3; L4: Lysate 4) at the different time points (T1: 72 h; T2: 120 h; T3: 240 h). Magnification ×20; bar 50 μm. Black triangle: Wound margins; black star: lymph-plasma-cell infiltration; black arrow: re-epithelialization.*

Cellular infiltration. Inflammatory cell infiltration was absent at T1 and T3, while a minimal, and short-lived, evenly distributed inflammatory cell infiltration was observed at T2.

The fibroblast infiltration was absent at T1, whereas at T2 and T3 a minimal and evenly distributed infiltration was observed.

Vascularisation. A scarce vascularisation was observed at all observation time points.

Dermal structure. The papillary dermis was absent at T1, whereas from T2 to T3 an early and progressive dermal development - from the peripheral injury margins towards the centre of the wound - was appreciated. The reticular dermis was very loose with thin collagen fibres at T1. At T2 *vs*. T1 the inter-fibrillary spaces were reduced. Nevertheless, at T3 the overall dermal organisation was similar to T1, though a blend of thin and thick collagen fibres was seen. The collagen fibres displayed a chaotic orientation at T1, whereas at T2 they displayed an orientation perpendicular to the skin's surface. At T3 the collagen fibres had adopted an orientation parallel to the skin's surface.

Lysate 2. Re-epithelialisation. A progressive advancement and multi-layered organisation of the re-epithelialisation front was appreciated at all observation time points. At T3, a complete lining of the central injury with a multi-layered epidermis, including the stratum corneum, was found. A basal keratinocyte melanin pigmentation was appreciated, too.

Cellular infiltration. A minimal peri-vascular inflammatory cell infiltration was found at T1. At T2, this pattern slightly increased. At T3, the amount of inflammatory cell infiltration was similar to T2, although an even distribution in the whole dermis was appreciated.

A minimal number of fibroblasts was seen at T1. At T2, the fibroblasts increased and were mainly distributed within the reticular dermis. At T3, the number of fibroblasts decreased *vs*. T2 and were distributed mainly in the papillary dermis.

Vascularisation. A scarce vascularisation was observed at all observation time points.

Dermal structure. The papillary dermis appeared immature at T1 and T2, whereas at T3 displayed a mature pattern. At T1, the reticular dermis was very loose, with a blend of thin and thick collagen fibres that displayed an orientation parallel to the surface of the skin. At T2, the reticular dermis appeared more compact, with a blend of thin and thick collagen fibres. The collagen fibres' orientation was perpendicular to the surface of the skin at this time. At T3, the collagen fibres' orientation changed to a direction parallel to the skin's surface. The dermal structure and compactness were the same as T2.

Lysate 3. Re-epithelialisation. A progressive advancement of the re-epithelialisation front was found from T1 to T2. At T3, a complete lining of the central injury with a multi-layered epidermis, without the stratum corneum, was appreciated.

Cellular infiltration. A moderate inflammatory perivascular cell infiltration was appreciated at T1. It slightly decreased at T2. At T3, the inflammatory cell infiltration increased and displayed an even distribution within the whole dermis. The fibroblast infiltration was minimal at all observation time points.

Vascularisation. A scarce vascularisation was observed at all observation time points.

Dermal structure. The papillary dermis was absent at T1 while some early and immature dermal structures appeared at T2 and T3. At T1, the reticular dermis was very loose, with a blend of thin and thick collagen fibres that displayed a chaotic organisation. At T2, the reticular dermis displayed a more hypertrophic pattern, with thick collagen fibres perpendicular to the skin's surface. At T3, the collagen fibres displayed a blend of thin and thick collagen fibres and returned to a chaotic organisation.

Lysate 4. Re-epithelialisation. A progressive advancement of the re-epithelialisation front was appreciated at T1 and T2. At these time points the multi-layered epithelial organisation was minimal. At T3, the epithelial lining of the central injury was complete. However, at T2 the multi-layered epithelium was missing the stratum corneum.

Cellular infiltration. A minimal and evenly distributed inflammatory cell infiltration was found at T1. It slightly increased at T2. At T3, the inflammatory cell infiltration decreased and displayed perivascular distribution within the whole dermis. The fibroblast infiltration was minimal at all observation time points.

Vascularisation. A scarce vascularisation was observed at all observation time points.

Dermal structure. The papillary dermis was absent at T1 while some early and immature dermal structures appeared at T2. At T3, an advanced development of the papillary dermis was seen. At T1 and T2, the reticular dermis was very loose, with a blend of thin and thick collagen fibres that displayed a chaotic organisation. At T3, the reticular dermis displayed a compact pattern, with thick collagen fibres perpendicular to the skin's surface.

Masson's Trichrome staining. Masson's Trichrome staining is shown in Figure 2.

Control (C). Masson's Trichrome staining displayed the same findings as with the haematoxylin and eosin staining at each observation time point. At T1 and T2, a blend of thin and thick collagen fibres was appreciated in the reticular dermis. However, these fibres displayed a chaotic organisation at T1 and an orientation perpendicular to the skin's surface at T2. At T3, a persisting blend of thin and thick collagen fibres was seen. At this time, the fibre orientation was perpendicular to the skin's surface.

Lysate 1. In the papillary dermis the findings were the same as with the haematoxylin and eosin staining at each observation time point. The reticular dermis at T1 displayed thin collagen fibres with a chaotic organisation. At T2 and T3, a blend of thin and thick collagen fibres was appreciated in the reticular dermis. The fibres displayed an orientation that was mainly perpendicular to the skin's surface.

Lysate 2. In the papillary dermis the findings were the same as with the haematoxylin and eosin staining at each observation time point. The reticular dermis at T1 displayed a blend of thin and thick collagen fibres with an orientation parallel to the skin's surface. Within the latter blend, a higher proportion of thick fibres was appreciated at this time. Some red-stained thick collagen fibres were found in the deep dermis below the puncture site. At T2, a blend of thin and thick collagen fibres was still seen but with inverted proportions: the thin collagen fibres prevailed over the thick ones. A higher amount of red-stained thick collagen fibres *vs*. the observation at T1 was appreciated. The fibres displayed an orientation perpendicular to the skin's surface. At T3, the blend of thin and thick collagen fibres was the same as at T2 although their orientation was parallel to the skin's surface.

Lysate 3. In the papillary dermis the findings were the same as with the haematoxylin and eosin staining at each observation time point. The reticular dermis at T1 displayed a blend of thin and thick collagen fibres with chaotic orientation. At T2, the collagen fibres turned into a keloid pattern with thick bundles featuring an orientation perpendicular to the skin's surface. At T3, the picture returned to a blend of thin and thick collagen fibres with an orientation perpendicular to the skin's surface.

Lysate 4. In the papillary dermis the findings were the same as with the haematoxylin and eosin staining at each observation time point. The reticular dermis at T1 displayed a blend of thin and thick collagen fibres with an orientation perpendicular to the skin's surface in the peripheral margins of the central puncture. Conversely, the collagen fibres were parallel to the skin's surface in the central and deep sites of the puncture. Furthermore, deep in the dermis, thick, red-stained collagen fibres with an orientation parallel to the skin's surface were appreciated. At T2, the collagen fibres were thick and featured a keloid pattern with chaotic orientation. At T3, the collagen fibres were thick and displayed an orientation perpendicular to the skin's surface.

Weigert staining. Weigert staining is shown in Figure 3.

Control (C). The same scarce number of elastic fibres was found at all observation time points. Nevertheless, a blend of long and short elastic fibres with an orientation perpendicular to the skin's surface was appreciated. The same pattern was displayed at T2 although a prevalence of fragmented elastic fibres was observed at this time. At T3, within the same pattern, a higher proportion of structured fibres with a parallel orientation to the skin's surface was appreciated.

Lysate 1. A progressive increase of structured fibres was seen from T1 to T2. At T3, the number of fibres was the same as at T2. The fibres displayed an orientation parallel to the skin's surface at T1 which then became perpendicular to the skin's surface at both T2 and T3.

Lysate 2. A large number of healthy and structured elastic fibres was found at all observation time points. The fibres progressively displayed an orientation parallel to the skin's surface that was complete by T3.

Lysate 3. A small number of elastic fibres was constantly found at all observation time points. At T1 and T2 the elastic fibres were long, while at T3 they displayed a higher degree of fragmentation. At T1 the fibres displayed an orientation perpendicular to the skin's surface. A chaotic orientation of the fibres was appreciated at T2 and T3.

Lysate 4. A small number of elastic fibres was constantly found at T1 and T2, whereas an increase was demonstrated at T3. Through all observation times, the orientation of the fibres changed progressively, until it became parallel to the skin's surface.

Ki-67 staining. Ki-67 staining is shown in Figure 4.

Control (C). At T1, a few Ki-67- stained nuclei were appreciated along the margins of the central puncture. At T2, the stained nuclei were observed within the re-epithelialisation front. At T3, a higher number of stained nuclei was observed within the incomplete epithelial lining of the central tissue.

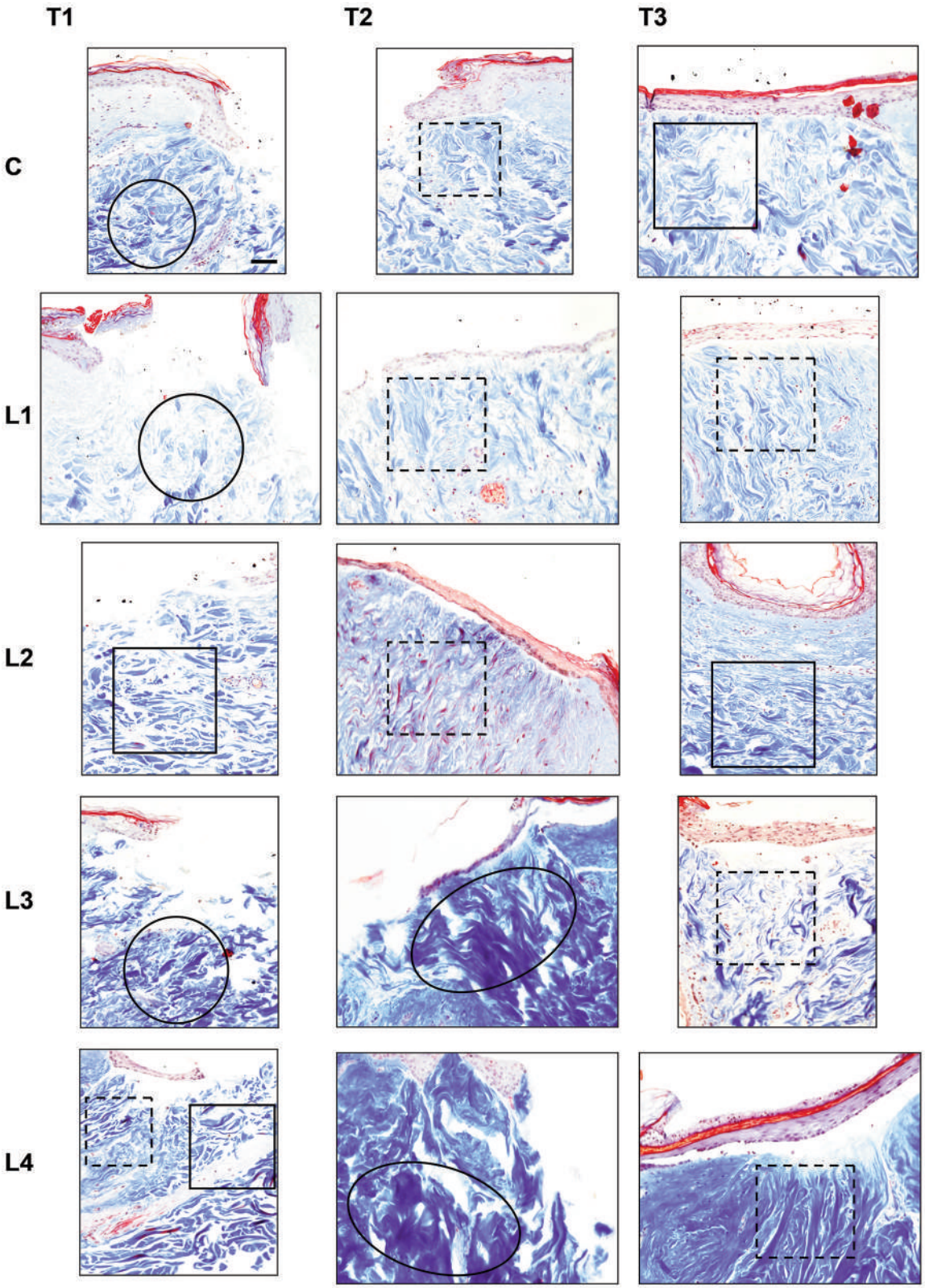

Figure 2. *Masson's trichrome staining in the different culture conditions (C: Control; L1: Lysate 1; L2: Lysate 2; L3: Lysate 3; L4: Lysate 4) at the different time points (T1: 72 h; T2: 120 h; T3: 240 h). Magnification ×20; bar 50 μm. Black circle: Chaotic reticular collagen fibres' orientation; black oval: hypertrophic dermis; square: parallel reticular collagen fibres' orientation; dotted line square: perpendicular reticular collagen fibres' orientation.*

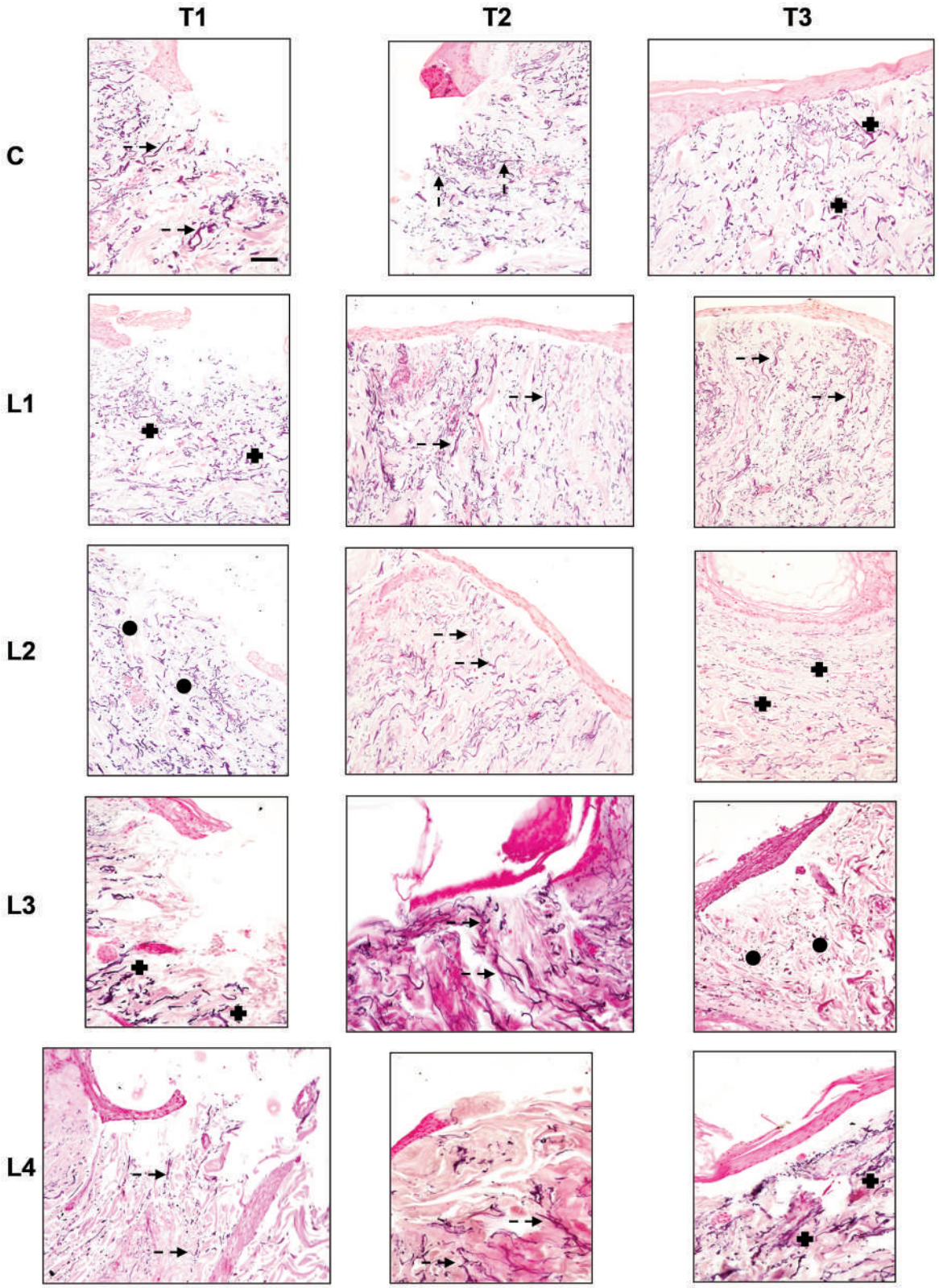

Figure 3. *Weigert staining in the different culture conditions (C: Control; L1: Lysate 1; L2: Lysate 2; L3: Lysate 3; L4: Lysate 4) at the different time points (T1: 72 h; T2: 120 h; T3: 240 h). Magnification ×20; bar 50 μm. Black circle: Poorly organized elastic fibres; black cross: parallel elastic fibres' orientation; dotted arrow: perpendicular elastic fibres' orientation.*

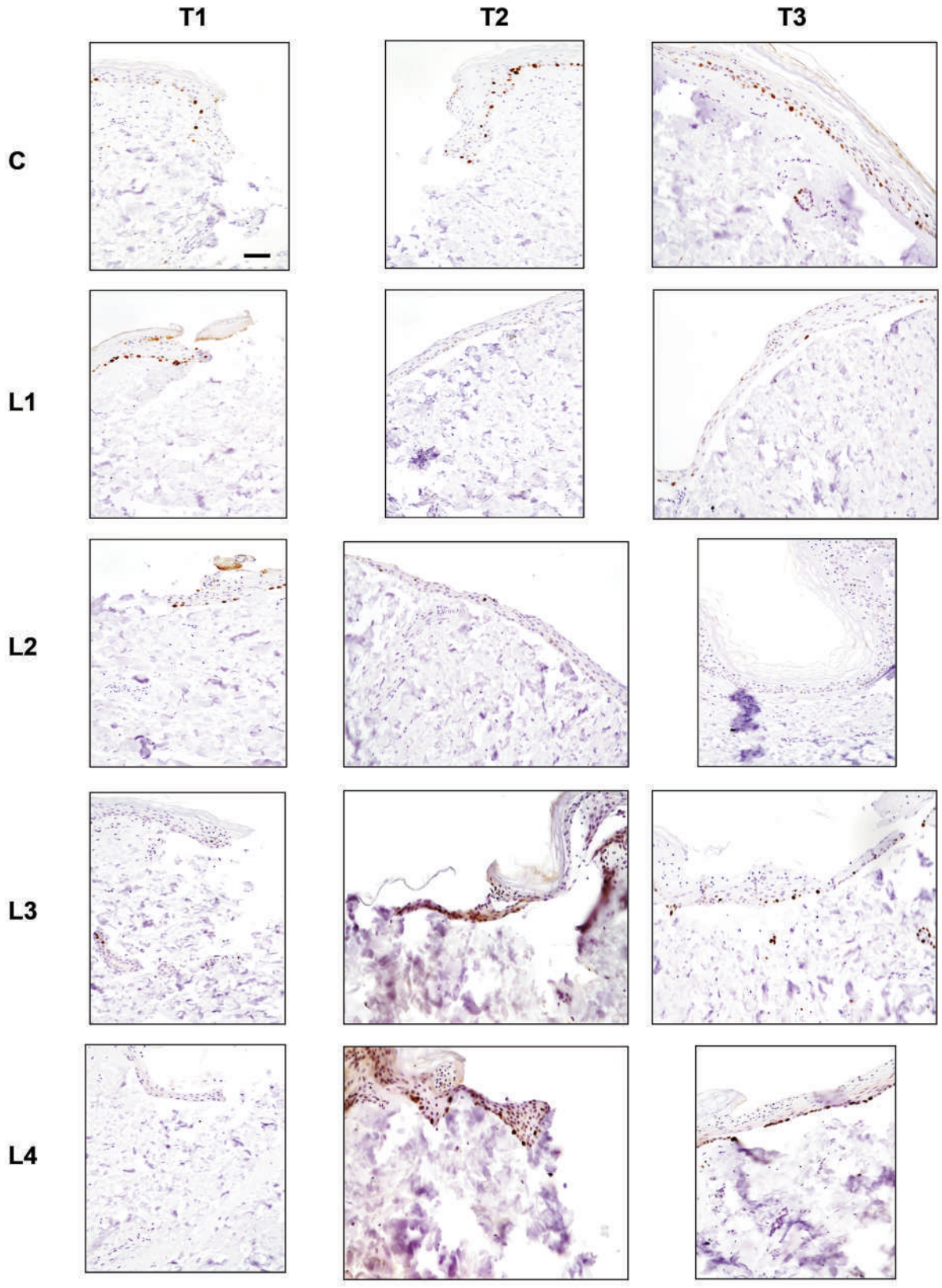

Figure 4. *Ki-67 staining in the different culture conditions (C: Control; L1: Lysate 1; L2: Lysate 2; L3: Lysate 3; L4: Lysate 4) at the different time points (T1: 72 h; T2: 120 h; T3: 240 h). Magnification ×20; bar 50 μm. Brown colour indicates the Ki-67-positive nuclei.*

Lysate 1. A progressive reduction of the number of Ki-67-stained nuclei was appreciated in all observation time points. At T1, the stained nuclei were observed in the re-epithelialisation front. At T3, a reduction of the number of stained nuclei was appreciated. These few nuclei were evenly distributed in the epithelial lining covering the centre of the sample.

Lysate 2. A progressive trend of reduction in the number of Ki-67-stained nuclei was appreciated at all observation time points. At T1, the stained nuclei were found within the re-epithelialisation front. At T2 and T3, the stained nuclei were observed within the complete epithelial lining of the central tissue.

Lysate 3. No Ki-67-stained nuclei were observed at T1. A small number of stained nuclei was appreciated at T2 and at T3. The stained nuclei were observed in the re-epithelialisation front in the early stages and within the complete epithelial lining by the end of the observation period.

Lysate 4. No Ki-67-stained nuclei were appreciated at T1. Many stained nuclei were observed at T2 and T3. At T2, the stained nuclei were localised both in the basal layer and in the superficial one within the re-epithelialisation front. At T3, the stained nuclei were appreciated in the basal layer but only within the complete epithelial lining of the central tissue.

Discussion

The trial demonstrated independent differential effects of the bacterial lysates extracted from the native non-pathogenic microflora of the Comano spring water, on the different parameters under study in an *ex-vivo* skin experimental wound model.

A complete re-epithelialisation of the experimental injuries at the end of the observation time was observed only in the samples cultured with L2, L3, and L4. In both L3 and L4. however, the epithelium was missing the stratum corneum. The regenerated epithelial lining displayed a complete and mature figure only in the samples cultured with L2. This picture matched the progressive decrease of epithelial cell proliferation recorded at the observation time points, as expected in a quickly completed maturation process.

The inflammatory infiltration demonstrated marked differences amongst the different experimental conditions. A progressive increase of the inflammatory infiltration was observed in the control samples at all observation time points. In the samples cultured with L1, the progressive inflammatory response was repressed from T2 onwards, thus indicating a marked anti-inflammatory effect induced by this bacterial product. In the samples cultured with L2, a progressive increase in the inflammatory infiltration was appreciated from T1 to T2, followed by a plateau, with no further increase till the end of the observation period. Conversely, in the samples cultured with L3 and L4, a short-lived anti-inflammatory effect was appreciated at the initial observation time and was followed by an increase in the inflammatory infiltration from the intermediate time period onwards, till the last one.

The fibroblast infiltration demonstrated a differential behaviour in the cultures with the bacterial lysates *vs*. the control ones. A progressive increase of the fibroblast infiltration was observed in the control samples at all observation time points. A similar progressive trend, although of lesser magnitude, was observed in the samples cultured with L1, whereas a scarce fibroblastic reaction was found in the samples cultured with the L3 and L4 lysates at all observation time points. The samples cultured with the L2 lysate, instead, displayed a smooth increase in the fibroblast infiltration - mainly located in the reticular dermis - up to the intermediate time point. This was followed by a smooth decrease and displacement in the papillary dermis by the end of the observation time. The dermal morphology displayed a progressive proliferation and maturation at all observation time points in the control samples. The orientation of the fibres was chaotic in the early stages. Progressively, this turned into an orientation perpendicular to the skin's surface and remained so at the end of the observation period. Such a picture was to be expected, just as in a typical wound healing process (13, 14).

Interestingly, the samples cultured with the L2 lysate displayed a well-organised structure and maturation of the whole dermis during the entire observation period. Throughout, the fibres always kept a regular orientation: parallel to the skin's surface in the early stage, perpendicular in the intermediate one and, again, parallel to the skin's surface by the end of the observation period. Unlike under the other experimental conditions, L2 never induced a chaotic pattern of collagen fibres. The samples cultured with the L1, L3, and L4 lysates displayed at some stage a chaotic orientation of the collagen fibres in the dermis with a clearly hypertrophic trait in the samples cultured with the L3 lysate (15, 16).

Elastic fibres were scarce in the control samples, as expected in any wound-healing process (17). The dermal cell proliferation matched the picture of the re-epithelialisation in the different experimental conditions at the different time points.

The combined inflammatory and fibroblast infiltration displayed different behaviours in the different experimental conditions. In the control samples, a progressive increase of both the inflammatory and fibroblast infiltration was noted at the observation time points, suggesting that such synergic cell proliferation represents the biological basis for a fibrotic reaction (13, 14).

In the samples cultured with the L2 lysate, the inflammatory cell response peaked in the intermediate period and remained

till the end of the observation time. The fibroblast infiltration seemed to match this trend with a peak and a selective placement in the reticular dermis at the intermediate period, followed by a smooth decrease and an elective distribution in the papillary dermis by the end of the observation time. Such a figure comprehensively suggests a fine combined-cell modulation, just as in a dermal regenerative process.

When considering the outcomes of the different observed parameters, the L2 bacterial lysate seems to provide a true regenerative boost and modulation in the experimental *ex-vivo* human skin wound model. Indeed, the samples cultured with this bacterial lysate demonstrated both an earlier and complete restoration of all the skin layers, the features of which were the closest to normal skin. The regenerated epidermis demonstrated a complete maturation, with both a stratum corneum and pigmentation in the basal layer, as observed in normal epidermis. Likewise, a mature papillary dermis covering a reticular dermis with both collagen and elastic fibres - regularly oriented parallel to the skin's surface - was observed but only in the cultures with the L2 bacterial lysate.

A consistent anti-inflammatory effect was displayed by the L1 lysate, yet such an action did not match a regenerative effect, thus suggesting that pathways for inflammation and regeneration within the wound healing process might be different (2, 18, 19).

This study aimed to identify within the native, rich, non-pathogenic microflora of Comano spring water single bacterial strains specifically promoting skin regeneration. The selection of the native bacterial strains to be assessed was based upon their anti-inflammatory effects, as our previous study on an *in-vivo* animal model demonstrated a reciprocal, opposite correlation between anti-inflammatory and regenerative effects (20). However, this research failed to confirm such a reverse correlation, suggesting that inflammation and regeneration might follow different paths within the wound healing process in the current experimental model. Currently, the replication of this study - for each of the remaining 177 bacterial strains currently identified within the non-pathogenic microflora of Comano spring water - with metagenomic techniques is not realistically feasible. Furthermore, these 177 bacterial strains feature many specific biological properties - other than the inflammation-modulating and/or regenerative effects (8). This study further suggests that the therapeutic power of spring water is not exclusively related to their mineral composition but may also be attributable to their native, non-pathogenic bacterial microflora, or, more likely, to their combined mineral and biological composition (4, 21-23).

Funding

The study was co-funded by the Fondazione per la Ricerca Scientifica Termale (FoRST), Rome, Italy (grant approved on 15/11/2017), and the Department of Clinical Surgical, Diagnostic and Pediatric Sciences, University of Pavia, Italy (grant approved on 18/01/2018).

Conflicts of Interest

The Authors have no conflicts of interest to declare in relation to this study.

Authors' Contributions

Conceptualization: AF and GN; Methodology: AF and GN; Formal analysis and investigation: MS, EMT, MMT, LV, OJ; Writing - original draft preparation: GN, AF, MS, MMT, OJ; Writing - review and editing: GN, AF, MMT and MS; Funding acquisition: AF and GN; Resources: GN and AF; Supervision: GN and AF.

Acknowledgements

The Authors wish to thank Morag McGhee (MA) and Eleanor Susan Lim (MA, Hons) for their contribution to the submission of this dissertation.

References

1 Kanno E, Kawakami K, Ritsu M, Ishii K, Tanno H, Toriyabe S, Imai Y, Maruyama R, Tachi M: Wound healing in skin promoted by inoculation with Pseudomonas aeruginosaPAO1: The critical role of tumor necrosis factor-α secreted from infiltrating neutrophils. Wound Repair Regen 19(5): 608-621, 2011. DOI: 10.1111/j.1524-475X.2011.00721.x

2 Lee HP, Choi YJ, Cho KA, Woo SY, Yun ST, Lee JT, Kim HJ, Lee KH, Kim JW: Effect of spa spring water on cytokine expression in human keratinocyte HaCaT cells and on differentiation of CD4(+) T cells. Ann Dermatol 24(3): 324-336, 2012. DOI: 10.5021/ad.2012.24.3.324

3 Kostarnoy AV, Gancheva PG, Logunov DY, Verkhovskaya LV, Bobrov MA, Scheblyakov DV, Tukhvatulin AI, Filippova NE, Naroditsky BS, Gintsburg AL: Topical bacterial lipopolysaccharide application affects inflammatory response and promotes wound healing. J Interferon Cytokine Res 33(9): 514-522, 2013. DOI: 10.1089/jir.2012.0108

4 Noizet M, Bianchi P, Galliano M, Caruana A, Brandner J, Bessou-Touya S, Duplan H: Broad spectrum repairing properties of an extract of *Aquaphilus dolomiae* on *in vitro* and *ex vivo* models of injured skin. J Eur Acad Dermatol Venereol 34(S5): 37-42, 2020. DOI: 10.1111/jdv.16477

5 Oliveira AS, Vaz CV, Silva A, Correia S, Ferreira R, Breitenfeld L, Martinez-de-Oliveira J, Palmeira-de-Oliveira R, Pereira C, Cruz MT, Palmeira-de-Oliveira A: *In vitro* evaluation of potential benefits of a silica-rich thermal water (Monfortinho Thermal Water) in hyperkeratotic skin conditions. Int J Biometeorol 64(11): 1957-1968, 2020. DOI: 10.1007/s00484-020-01986-x

6 Nicoletti G, Saler M, Pellegatta T, Malovini A, Faga A, Scalise A, Riva F: Effects of a spring water on human skin fibroblasts *in vitro* cultures: preliminary results. Acta Vulnologica 14(4): 196-201, 2016.

7 Nicoletti G, Saler M, Pellegatta T, Tresoldi MM, Bonfanti V, Malovini A, Faga A, Riva F: *Ex vivo* regenerative effects of a

spring water. Biomed Rep 7(6): 508-514, 2017. DOI: 10.3892/br.2017.1002

8 Nicoletti G, Corbella M, Jaber O, Marone P, Scevola D, Faga A: Non-pathogenic microflora of a spring water with regenerative properties. Biomed Rep 3(6): 758-762, 2015. DOI: 10.3892/br.2015.507

9 Pedron R, Esposito A, Bianconi I, Pasolli E, Tett A, Asnicar F, Cristofolini M, Segata N, Jousson O: Genomic and metagenomic insights into the microbial community of a thermal spring. Microbiome 7(1): 8, 2019. DOI: 10.1186/s40168-019-0625-6

10 Nicoletti G, Saler M, Tresoldi MM, Faga A, Benedet M, Cristofolini M: Regenerative effects of spring water-derived bacterial lysates on human skin fibroblast in *in vitro* culture: preliminary results. J Int Med Res 47(11): 5777-5786, 2019. DOI: 10.1177/0300060519880371

11 Nicoletti G, Saler M, Villani L, Rumolo A, Tresoldi MM, Faga A: Platelet rich plasma enhancement of skin regeneration in an *ex-vivo* human experimental model. Front Bioeng Biotechnol 7: 2, 2019. DOI: 10.3389/fbioe.2019.00002

12 Nakamura M, Rikimaru T, Yano T, Moore KG, Pula PJ, Schofield BH, Dannenberg AM: Full-thickness human skin explants for testing the toxicitiy of topically applied chemicals. J Invest Dermatol 95(3): 325-332, 1990. DOI: 10.1111/1523-1747.ep12485073

13 Rippa AL, Kalabusheva EP, Vorotelyak EA: Regeneration of dermis: Scarring and cells involved. Cells 8(6): 607, 2019. DOI: 10.3390/cells8060607

14 Rodrigues M, Kosaric N, Bonham CA, Gurtner GC: Wound healing: a cellular perspective. Physiol Rev 99(1): 665-706, 2019. DOI: 10.1152/physrev.00067.2017

15 Zhang J, Li Y, Bai X, Li Y, Shi J, Hu D: Recent advances in hypertrophic scar. Histol Histopathol 33(1): 27-39, 2018. DOI: 10.14670/HH-11-908

16 Wang ZC, Zhao WY, Cao Y, Liu YQ, Sun Q, Shi P, Cai JQ, Shen XZ, Tan WQ: The roles of inflammation in keloid and hypertrophic scars. Front Immunol 11: 603187, 2020. DOI: 10.3389/fimmu.2020.603187

17 Zhang X, Alanazi YF, Jowitt TA, Roseman AM, Baldock C: Elastic fibre proteins in elastogenesis and wound healing. Int J Mol Sci 23(8): 4087, 2022. DOI: 10.3390/ijms23084087

18 Gerencsér G, Szabó I, Szendi K, Hanzel A, Raposa B, Gyöngyi Z, Varga C: Effects of medicinal waters on the UV-sensitivity of human keratinocytes – a comparative pilot study. Int J Biometeorol 63(10): 1417-1423, 2019. DOI: 10.1007/s00484-019-01759-1

19 Silva A, Oliveira AS, Vaz CV, Correia S, Ferreira R, Breitenfeld L, Martinez-de-Oliveira J, Palmeira-de-Oliveira R, Pereira CMF, Palmeira-de-Oliveira A, Cruz MT: Anti-inflammatory potential of Portuguese thermal waters. Sci Rep 10(1): 22313, 2020. DOI: 10.1038/s41598-020-79394-9

20 Faga A: Effects of thermal water on skin regeneration. Int J Mol Med 29(5): 732-40, 2012. DOI: 10.3892/ijmm.2012.917

21 Mahe YF, Perez MJ, Tacheau C, Fanchon C, Martin R, Rousset F, Seite S: A new Vitreoscilla filiformis extract grown on spa water-enriched medium activates endogenous cutaneous antioxidant and antimicrobial defenses through a potential Toll-like receptor 2/protein kinase C, zeta transduction pathway. Clin Cosmet Investig Dermatol 6: 191-196, 2013. DOI: 10.2147/CCID.S47324

22 Aries MF, Duplan H, Hernandez-Pigeon H, Galliano MF, Castex-Rizzi N, Bessou-Touya S, Nguyen T: I-modulia, an Aquaphilus dolomiae extract, stimulates innate immune response through Toll-like receptor activation. J Am Acad Dermatol 70(5): AB63, 2014. DOI: 10.1016/j.jaad.2014.01.261

23 Lestienne F, Viodé C, Ceruti I, Carrere S, Bessou-Touya S, Duplan H, Castex-Rizzi N: Cutaneous sensitivity modulation by Aquaphilus dolomiae extract-G3 on *in vitro* models of neuro-inflammation. J Eur Acad Dermatol Venereol 34 Suppl 5: 43-48, 2020. DOI: 10.1111/jdv.16641

Received June 14, 2023
Revised July 19, 2023
Accepted July 24, 2023